Simulation of Screw Dislocation Motion in Iron by Molecular Dynamics Simulations

Christophe Domain and Ghiath Monnet

Electricité de France, Research and Development, Department MMC, Les Renardières, F-77818 Moret sur Loing, France

(Received 3 August 2005; published 17 November 2005)

Molecular dynamics (MD) simulations are used to investigate the response of $a/2\langle 111\rangle$ screw dislocation in iron submitted to pure shear strain. The dislocation glides and remains in a (110) plane; the motion occurs exclusively through the nucleation and propagation of double kinks. The critical stress is calculated as a function of the temperature. A new method is developed and used to determine the activation energy of the double kink mechanism from MD simulations. It is shown that the differences between experimental and simulation conditions lead to a significant difference in activation energy. These differences are explained, and the method developed provides the link between MD and mesoscopic simulations.

DOI: 10.1103/PhysRevLett.95.215506 PACS numbers: 61.72.Lk, 61.72.Bb, 61.82.Bg

Low temperature deformation of body centered cubic metals is known to be thermally activated and to be controlled by the behavior of the $a/2\langle 111\rangle$ screw dislocations; for a review, see [1,2]. Dislocations of other characters move quickly at lower stresses, generating long screw dislocations. This explains the predominant screw character in the microstructure observed at low temperature [3]. The motion of screw dislocations is historically associated with the double kink (DK) mechanism [4,5], but the details about the activation process are still a debated question. There is a large discrepancy in experimental results on the evolution of the critical resolved shear stress (CRSS) as a function of temperature. Several reasons can be invoked: the large sensitivity to solid-solution content [6], the non-Schmid law behavior [7], and the large extent of stage 0 at low temperature [8]. The case of iron is even more problematic, because it is extremely sensitive to the carbon content.

In this context, molecular dynamics (MD) simulations are a powerful and alternative tool to explore specific microscopic phenomena. However, the crucial point in MD simulations is still the empirical atomic potential used to describe atomic interactions. The embedded atom method (EAM) potential developed by Ackland *et al.* [9] for iron has been used for a long time to investigate dislocation related properties [10–13]. This potential leads to a core structure with a threefold symmetry for the screw dislocation which is in disagreement with *ab initio* results [14], for which the core is compact with no preferential spreading, as well as obtained in Ta, W, or Mo [15]. Marian *et al.* [13] have simulated the dynamical behavior of such a screw dislocation, but neither the temperature dependence of the CRSS has been discussed explicitly nor a quantitative description of the dislocation motion was given. However, the main discrepancy is still the very large Peierls stress obtained by MD [10,13] which is very far from experimental values.

In this Letter, we use the recent EAM potential derived by Mendelev *et al.* [16] to characterize the exact response of a $a/2\langle 111\rangle$ screw dislocation in iron submitted to a pure shear load at different temperatures. A specific method is developed to determine, under dynamic conditions, the critical stress associated to the DK mechanism. We present in this work the first discussion of the stress values obtained in MD and the exact link to experimental results.

The first advantage of the Mendelev EAM potential for iron [16], which was partially fitted on *ab initio* results, is that it predicts for the first time the compact relaxed core structure of the screw dislocation in agreement with the structure obtained by *ab initio*; see Fig. 1. The dislocation line is placed at the center of the simulation box, periodic boundary conditions are applied along the line, and surfaces are present in the two other directions. The dislocation is constructed by applying to all the atoms the isotropic elastic solution of the displacement field. The core structure given by the EAM potential is obtained by quenching the atomic positions, while, by *ab initio*, the conjugate gradient algorithm was used except for the outer atomic shell, which was fixed. Our *ab initio* calculations were performed using the VASP code [17], with a 75 atom supercell. The projector augmented wave pseudopotential [18] from the VASP library was used within the spin polarized generalized gradient approximation. The core structure obtained (Fig. 1) is similar to the one of Frederiksen and Jacobsen's *ab initio* calculations [14], which were

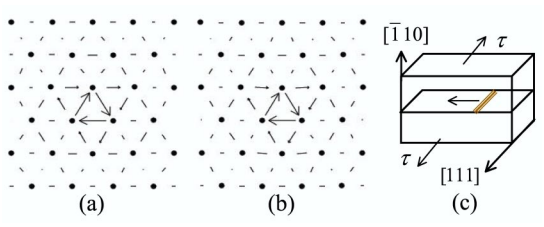

FIG. 1 (color online). (a) Relaxed core structure by *ab initio*, (b) relaxed core structure with Mendelev *et al.* potential [16], and (c) MD simulation box and boundary conditions.

done with a network of screw dislocation dipoles and periodic boundary conditions.

For the study of the dislocation motion at a given temperature, MD simulations are performed at constant strain rate using the DYMOKA code. The screw dislocation is initially created at the center of the box. Periodic boundary conditions are applied in the [111] direction, free surfaces in the $[11\bar{2}]$ direction, and four adjacent atomic planes are fixed in the upper and lower $(\bar{1}10)$ surfaces. The system size is 9.9 nm along the [111] direction, 7.3 nm along $[\bar{1}10]$, and 14.1 nm along $[11\bar{2}]$; see Fig. 1. The fixed block of atoms is then translated in the [111] direction, corresponding to a deformation rate close to 1.5×10^7 s^{-1}. Before starting the deformation, the mobile atoms are thermalized at the chosen temperature. The shear stress is calculated from the component of the force on the fixed atoms parallel to the Burgers vector b.

All MD simulations show that the screw dislocation glides in the $(\bar{1}10)$ plane at all investigated temperatures. The motion of the screw dislocation occurs through the nucleation and the propagation of a DK along the dislocation line, as shown in Fig. 2. The arrow method developed by Vitek, Perrin, and Bowen [19] was used to localize the dislocation core. Only pairs of atoms for which the relative displacement in the [111] direction is equal or larger than $b/3$ are represented in Fig. 2.

A DK corresponds to a jump of a dislocation segment to an adjacent triangle in the [111] projection. Systematically, every DK is followed by another DK putting the dislocation in a second adjacent triangle, exactly as predicted 30 years ago [1]. The reason is that a single DK moves the dislocation from a "soft" position, with a low core energy, to a "hard" position, which is unstable in dynamic conditions. A second DK is then rapidly nucleated, putting back the dislocation in the soft configuration. The velocity of the kink propagation is found close to the sound velocity, confirming that the controlling process is the nucleation of the DK. In Fig. 3 we show a typical shear-stress (τ) shear-strain (γ) curve at constant strain rate. It starts by an elastic response corresponding to 73 GPa for the shear modulus, followed by a region of fluctuating stress with several local maxima. Simulations being carried out at constant strain rate, the stress decreases after the nucleation of one or more DKs. The fluctuation of the values of the stress maxima is certainly due to the probabilistic feature of collective jumps of atoms. One can also note a tendency of the stress to decrease in the plastic stage. These features reveal the difficulty to estimate from MD simulations an unambiguous value of the critical stress. The following procedure is proposed and developed in the present work.

First, when it moves from the center of the simulation box, the dislocation is submitted to the attraction of the free surface in front of it. This is equivalent to adding an extra stress component τ_s, which leads to the decrease of the elastic energy of the dislocation. MD simulation can be used to evaluate this energy by determining the potential energy E, as a function of the position x, of the dislocation under zero applied stress. Then the real or effective stress τ_{eff} seen by the dislocation can be written as follows:

$$\tau_{\text{eff}} = \tau + \tau_s = \tau - \frac{1}{bL}\frac{\partial E}{\partial x}, \tag{1}$$

where L is the length of the dislocation. This correction was found to be necessary to compensate the decrease of the applied stress when the dislocation approaches the free surface of the simulation box; see Fig. 3. Second, because of the stress fluctuation, a special approach to determine the critical effective stress (CES) value τ_c is derived. This value is one of the most important results of MD simulations, called MD-CES in the following. It can and should be compared to the thermal component of the CRSS obtained experimentally, called also critical effective stress, exp-CES in the following. The frequency of the collective jump increases with stress, but, during the incubation time, the probability depends on the stress history. Now all theoretical models [5,20–22] assume that the probability of DK nucleation is proportional to the number of nucleation sites along the dislocation line, i.e., proportional to the length of the screw dislocation segment L. These models also assume that the most important role of stress is to

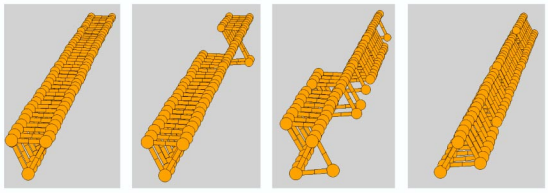

FIG. 2 (color online). Nucleation and propagation of a DK at 75 K from the soft to the hard position from right to left.

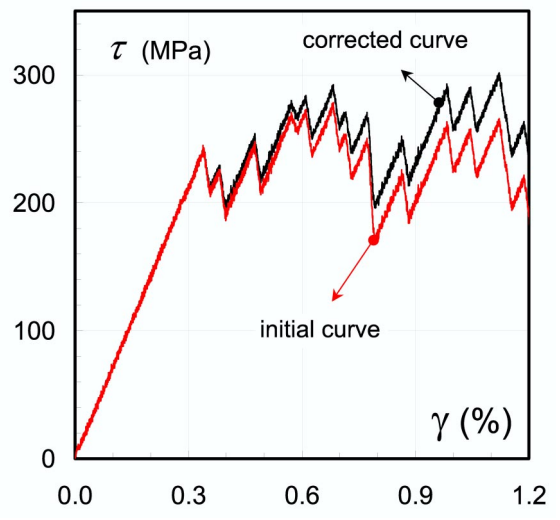

FIG. 3 (color online). Typical τ-γ curve. Simulation made at 300 K and 1.5×10^7 s^{-1} strain rate.

decrease the activation energy ΔG. If the latter is expanded in a Taylor's series about an appropriate τ value, we have $\Delta G = B - V\tau_{\text{eff}}$, where B is constant and V is the activation volume. Applied to our MD simulations, these models provide the following formula relating the average velocity v to τ_c:

$$v = AL\exp\left(-\frac{B - V\tau_c}{kT}\right) = AL\left\langle\exp\left(-\frac{B - V\tau_{\text{eff}}}{kT}\right)\right\rangle, \quad (2)$$

where A is constant almost independent of stress, k is the Boltzmann constant, T is the absolute temperature, and $\langle..\rangle$ denotes the mean value. L is assumed to be constant, since no more than one DK is generated simultaneously in our MD simulations. In the first approximation, V can be considered as constant in the plastic regime, e.g., for γ between 0.3 and 1.2 in Fig. 3, because of the small stress fluctuation. Consequently, the critical stress value can be given by:

$$\tau_c = \frac{kT}{V}\ln\left\langle\exp\left(\frac{V\tau_{\text{eff}}}{kT}\right)\right\rangle. \quad (3)$$

From experimental investigations on single crystals [23,24], V was found close to 20 b^3 for the typical stress values of our simulations; see Fig. 3. Therefore, Eq. (3) can be used to provide a good estimation of the CES from MD simulations carried out under the fixed strain rate.

In order to investigate the role of thermal activation on the DK mechanism, MD simulations were carried out at six different temperatures. The evolution of the critical stress obtained by Eqs. (2) and (3) is shown in Fig. 4. The figure reveals a strong dependency of the critical effective stress on temperature. Two deviations from experimental results can be noted. The dependency on temperature is less marked in MD simulations than experimentally, and the values of MD-CES are significantly larger than those of exp-CES, especially at high temperature. In addition, for temperatures larger than 300 K, exp-CES is independent of temperature. An athermal plateau is believed to exist for $T > 300$ K, which is not reproduced by MD simulations. In the following, we will see that, from a physical point of view, these discrepancies are only apparent. The deviation is due to the dynamic and probabilistic features of the DK mechanism.

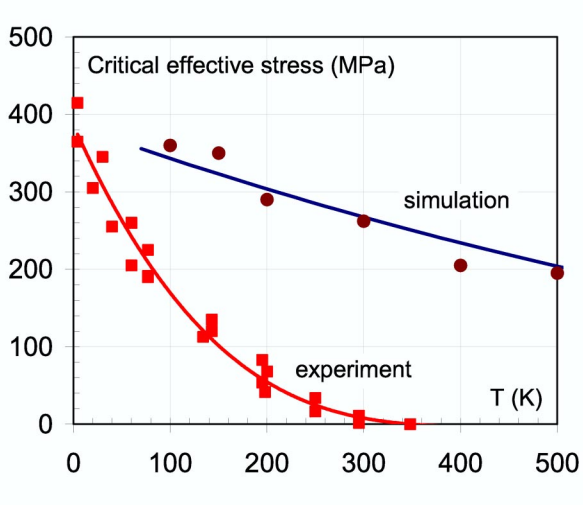

FIG. 4 (color online). Evolution of the effective critical stress on the (110) plane as a function of the temperature at fixed strain rate. Squares denote the experimental values (exp-CES) [7,23,27] and circles denote MD simulation results (MD-CES). Description of solid lines is given in the text.

From Eq. (2), we can see that, at a given temperature, among τ_c, L, and v, there are only two independent variables. In MD simulations and in experiments, L and v are fixed, and τ_c is measured. The length and velocity of the screw dislocation have to be evaluated in order to make a quantitative link between MD and experiments. The activation free Gibbs energy is composed of an activation enthalpy ΔH and an entropy ΔS. The later was evaluated [25] using the Schoeck's correction [26] and its contribution found to be less than 5% of the activation energy; it is thus neglected. However, the relation between the CES and ΔH is not explicit, since the force-distance curve and the saddle configuration during the jump cannot be obtained directly from experiment. This is why we consider first the dependency of ΔH on L and v and, then, correlate MD and experimental values of the CES. The Orowan equation, expressing the strain rate $\dot{\gamma}$, as a function of the velocity and density ρ of mobile dislocations, $\dot{\gamma} = bv\rho$, allows one to evaluate the experimental velocity v_{exp}. At the end of deformation stage 0 [3], the dislocation microstructure is essentially formed of screw dislocations and the corresponding density is close to 10^{12} m^{-2}. Since experiments were carried out at 10^{-4} s^{-1} shear rate [7,23,27], v_{exp} is of the order of 0.4 μm/s. As for the segment length, L_{exp} is close to the average dislocation spacing of almost 1 μm. In MD simulations, L_{sim} is equal to 9.9 nm and the average velocity v_{sim} is found close to 4 m/s. Consequently, because of the length and the velocity of the screw dislocation in MD simulations, the corresponding activation enthalpy is different from that measured in tensile tests. By applying Eq. (2), for both experiment and simulations, one gets:

$$\Delta H_{\text{sim}} = \Delta H_{\text{exp}} + kT\ln\frac{v_{\text{exp}}L_{\text{sim}}}{v_{\text{sim}}L_{\text{exp}}}. \quad (4)$$

The value of the logarithm in the right-hand side of Eq. (4) is always negative. This means that carrying out MD simulations with the conditions mentioned above deprives the process of a certain amount of thermal energy close to $21kT$. This loss in activation energy implies obviously a large increase of the shear stress. This is why the values of critical stresses found in MD simulations are large compared to experiment; see Fig. 4. The difference can be even more quantified if we consider the following reasoning. The activation enthalpy was experimentally found to be proportional to the temperature [24,28]

$\Delta H_{\mathrm{exp}} = CkT$. In experimental investigation [7], C was found close to 25. Equation (4) then allows us to deduce the activation enthalpy in MD simulations, $\Delta H_{\mathrm{sim}} = 4kT$. This energy is relatively small. It explains the less pronounced decrease of MD-CES as a function of temperature; see Fig. 4. Furthermore, the temperature T_c, at which the athermal plateau should start in MD simulations, can be given by $\Delta H_0/(4k) = 2419$ K, where ΔH_0 is the total energy barrier, estimated experimentally [25] to 0.84 eV. In other terms, no athermal plateau can be detected in MD simulations, because of the specificity of the MD simulation conditions.

Using Eq. (4), it is possible to establish the relation between MD-CES and exp-CES. Equation (4) indicates that the difference between ΔH_{exp} and ΔH_{sim} is proportional to the temperature. When an MD simulation is performed at a given temperature T, the activation enthalpy equals $4kT$. This quantity is the same as the activation energy measured experimentally at $(4kT/25k) = 0.16T$. Similarly, the CES measured experimentally at a given temperature T should be close to that obtained by MD at a temperature equals $1/0.16T = 6.25T$.

In order to check out this correlation, two solid lines were added to Fig. 4. The first one, $f(T)$, is simply the best fit of experimental results, and the second one is the function $f(0.16T)$. It can be clearly seen that the curve $f(0.16T)$ describes quite well the MD results. It is possible to explain and predict to a very good approximation the MD results by considering the thermal activation nature of the DK mechanism. *Vice versa*, the theory of the DK mechanism expressed in Eq. (2) is thus confirmed by MD simulations. As shown in our discussion, it is possible to connect easily atomic level description to the mesoscopic picture of the motion of the $a/2\langle 111\rangle$ screw dislocation.

In conclusion, using the Mendelev potential as the only input data, MD simulations are found to reproduce in good agreement experimental observations: The motion of the screw dislocation occurs by DK in the (110) plane, and the evolution of the obtained critical stress can easily be linked to the CES measured experimentally. This agreement is the first one reported in the literature and represents a mutual validation of theories and MD simulations of the double kink mechanism.

This work is funded by the European PERFECT project (No. FI6O-CT-2003-508840).

[1] L. P. Kubin, Reviews on the Deformation Behavior of Materials **1**, 243 (1976).
[2] J. W. Christian, Metall. Trans. A **14A**, 1237 (1983).
[3] F. Louchet and L. P. Kubin, Acta Metall. **23**, 17 (1975).
[4] A. Seeger and P. Schiller, Acta Metall. **10**, 348 (1962).
[5] J. E. Dorn and S. Rajnak, Trans. Metall. Soc. AIME **230**, 1052 (1964).
[6] T. Takeuchi, Trans. Iron Steel Inst. Jpn. **8**, 251 (1968).
[7] W. A. Spitzig and A. S. Keh, Acta Metall. **18**, 611 (1970).
[8] H. D. Solomon and C. J. McMahon, Jr., Acta Metall. **19**, 291 (1971).
[9] G. J. Ackland, D. J. Bacon, A. F. Calder, and T. Harry, Philos. Mag. A **75**, 713 (1997).
[10] M. Wen and A. H. W. Ngan, Acta Mater. **48**, 4255 (2000).
[11] T. Harry and D. J. Bacon, Acta Mater. **50**, 195 (2002).
[12] Y. N. Osetsky and D. J. Bacon, J. Nucl. Mater. **323**, 268 (2003).
[13] J. Marian, W. Cai, and V. V. Bulatov, Nat. Mater. **3**, 158 (2004).
[14] S. L. Frederiksen and K. W. Jacobsen, Philos. Mag. A **83**, 365 (2003).
[15] S. Ismail-Beigi and T. A. Arias, Phys. Rev. Lett. **84**, 1499 (2000); C. Woodward and S. I. Rao, Phys. Rev. Lett. **88**, 216402 (2002).
[16] M. I. Mendelev, S. W. Han, D. J. Srolovitz, G. J. Ackland, D. Y. Sun, and M. Asta, Philos. Mag. **83**, 3977 (2003).
[17] G. Kresse and J. Hafner, Phys. Rev. B **47**, R558 (1993); **49**, 14 251 (1994); G. Kresse and J. Furthmüller, Phys. Rev. B **54**, 11 169 (1996); Comput. Mater. Sci. **6**, 15 (1996).
[18] G. Kresse and D. Joubert, Phys. Rev. B **59**, 1758 (1999); P. E. Blöchl, Phys. Rev. B **50**, 17 953 (1994).
[19] V. Vitek, R. C. Perrin, and D. K. Bowen, Philos. Mag. **21**, 1049 (1970).
[20] F. A. Smidt, Acta Metall. **17**, 381 (1969).
[21] F. Louchet and L. P. Kubin, Phys. Status Solidi A **56**, 169 (1979).
[22] M. Tang, L. P. Kubin, and G. R. Canova, Acta Mater. **46**, 3221 (1998).
[23] E. Kuramoto, Y. Aono, and K. Kitajima, Scr. Metall. **13**, 1039 (1979).
[24] W. A. Spitzig, Mater. Sci. Eng. **12**, 191 (1973).
[25] W. A. Spitzig and A. S. Keh, Acta Metall. **18**, 1021 (1970).
[26] G. Schoeck, Phys. Status Solidi **8**, 499 (1965).
[27] D. F. Stien, J. R. Low, and A. U. Seybolt, Acta Metall. **11**, 1253 (1963).
[28] M. Cagnon, Philos. Mag. **24**, 1465 (1971).